Published in final edited form as:
Dalton Trans. 2009 July 7; (25): 5023–5028. doi:10.1039/b904113c.

Synthesis, characterization and structure of a low coordinate desoxomolybdenum cluster stabilized by a dithione ligand†

Eranda Perera and **Partha Basu***
Department of Chemistry and Biochemistry, Duquesne University, Pittsburgh, PA 15282, USA.

Abstract

Using an oxidized state of a dithiolene ligand, diisopropylpiperazine-2,3-dithione (i-Pr_2Pipdt), two monooxo-molybdenum complexes have been synthesized. From one of them, a desoxomolybdenum cluster, $[(i\text{-}Pr_2Pipdt)Mo]_4[BF_4]_4$ has been prepared. The molecular structure of this cluster reveals metal-metal interactions and weak coordination by the BF_4 anion.

Introduction

The chemistry of metallodithiolenes has long been investigated, because of their potential applications in nonlinear optics, light driven information devices, laser dyes, and sensors.[1-4] A general approach to tune the molecular properties involves incorporation of suitable substituents as well as changing the metal ions. The former approach has resulted in molecular superconductors.[5-7] While the homoleptic 1,2-dithiolene mononuclear complexes resulted in a range of geometry from square planar to trigonal prismatic, structures and properties of the polynuclear complexes of 1,2-dithiolene are yet to be fully developed,[8] although such complexes are of interest as promising materials.[7,9]

Polynuclear transition metal complexes, including those of molybdenum continue to garner interest as a vehicle to understand catalysis at metal surfaces.[1,3,4,7,10-14] Of these, geometric and electronic structures of compounds with metal–metal bonds have been investigated.[15]

Molybdenum complexes of 1,2-dithiolene are of interest as they constitute the active sites of pterin-containing molybdenum enzymes.[16] These enzymes often catalyze a net oxygen atom transfer (OAT) reaction at the molybdenum center. Unlike the enzymatic systems, OAT reactions in model complexes encounter pervasive dinucleation reactions leading to μoxo-bridged complexes, which constitute the majority of the polynuclear complexes of 1,2-dithiolene.[17] This process is thermodynamically favorable, as self-assembly of lower nuclearity complexes lead to polynuclear compounds, and may provide an entry to desired higher nuclearity complexes.

The 1,2-dithiolene ligands are redox non-innocent and can exhibit a variety of redox states, which can influence the overall properties of the metal center. We are interested in understanding the properties of the metal complexes with an oxidized form of the ligand. To this end, we reported solvatochromic properties of a lower-valent molybdenum complex of an oxidized dithiolene, $(Me_2Pipdt)Mo(CO)_4$, (where Me_2Pipdt is *N*,*N*′-piperazine-2,3-dithione);[18] the reduced form of the ligand is highly air sensitive.[19] A systematic investigation of higher

†CCDC reference numbers 722174 & 722175. For crystallographic data in CIF or other electronic format see DOI: 10.1039/b904113c

basu@duq.edu .

valent molybdenum complexes of the oxidized ligand is yet to be described. Herein we report the synthesis and characterization of two oxo-molybdenum complexes $[(i\text{-}Pr_2Pipdt)_2MoOCl][MoOCl_4]$ (**1a**), and $[(i\text{-}Pr_2Pipdt)_2MoOBF_4][BF_4]$ (**1b**) (where, $i\text{-}Pr_2Pipdt$ = diisopropylpiperazine-2,3-dithione) (Scheme 1). This constitutes the first report of an oxo-molybdenum(IV) dithione complex. In the presence of pyridine, $[(i\text{-}Pr_2Pipdt)_2MoOBF_4][BF_4]$ forms an unique desoxo-molybdenum cluster, $[(i\text{-}Pr_2Pipdt)Mo]_4[BF_4]_4$ (**2**), which has been spectroscopically and analytically characterized. In addition to the spectroscopic characterization, we report the structure of this cluster.

Experimental

Syntheses of molybdenum complexes were carried out in oxygen-free dry argon atmospheres using dry degassed solvents. The ligand, diisopropylpiperazine-2,3-dithione ($i\text{-}Pr_2Pipdt$), was synthesized in air.[20,21] Solvents were purchased either from Aldrich Chemical Co. or Acros Organics and were purified by distillation as follows: acetonitrile from CaH_2, followed by Li_2CO_3–$KMnO_4$ and finally from P_2O_5; CH_2Cl_2 and $CHCl_3$ from CaH_2; diethyl ether and toluene from sodium benzophenone; methanol from sodium ethoxide. $MoCl_5$, *N*,*N*-dimethyl ethylene diamine, *N*,*N*-diisopropyl ethylene diamine and Lawesson's reagent were purchased from Aldrich and used without purification. Diethyl oxalate was purchased from Acros Organics and used as received.

Spectroscopic/Spectrometric measurements

UV-Visible spectra were recorded on a modified temperature-controlled Cary 14 spectrophotometer or a temperature controlled Cary 3 spectrophotometer. ^1H, ^{19}F and ^{13}C NMR spectra were collected using either a Bruker 500 MHz or 400 MHz spectrometer. IR spectra were recorded in reflection mode on a Thermo Electron corporation Nicolet 380 spectrometer with neat samples. Elemental analysis was performed by Midwest Microlab LLC, Indiana, IL. All mass spectra were collected in a Micromass ZMD quadrupole spectrometer equipped with an electrospray ionization (ESI) source both negative and positive ion mode, using acetonitrile as the mobile phase. In order to get the molecular ion peak the capillary and the cone voltages were varied between 3.0–4.0 kV and 5–55 V respectively. The desolvation temperature was set at 100°C and the source bath temperature was set at 80°C.

X-ray structure determination

Molecular structures of the ligand, $i\text{-}Pr_2Pdt$, and the cluster, **2**, have been determined by X-ray crystallography. Here we discuss the details of structure **2** and use the structure of the ligand[19] for comparison in the Discussion section. X-ray quality crystals were grown from slow diffusion of ether into the acetonitrile solutions. Data collection was conducted on a Bruker SMART Apex II diffractometer with a graphite monochromator for Mo K_α radiation at 0.71073 Å. A total of 16 707 reflections were collected and 6216 reflections satisfied the condition $I > 3\sigma(I)$ and were used for the structure determination. Absorption correction was performed using SADABS.[22] Based on the systematic absences the XPREP determined space group and the structure and was solved in the triclinic crystal system with the space group *P* (-1). The structure was solved using the Patterson method in SHELX-97. The structure was refined using full matrix least square method.[23] All non hydrogen atoms were refined anisotropically and the hydrogen atoms were added using the riding model. On the basis of 6216 independent reflections, the structure was refined to $R = 0.046$ with GOF = 1.085. Details of the structure determination = are listed in Table 1.

Synthesis of $[(i\text{-}Pr_2Pipdt)_2MoOCl][MoOCl_4]$ (1a)—110 mg (0.64 mmoles) of $MoCl_5$ and 5 mL of dry degassed THF were equilibrated separately at −78°C. The cold THF was added drop wise to $MoCl_5$ to form a grass green colored slurry of $MoOCl_3(THF)_2$. To this slurry, 175

mg (1.3 mmoles) of *N*,*N* diisopropyl piperazine-2,3-dithione was added, and the reaction mixture was stirred for 4 h. With the addition of the ligand, the solution color changed to dark brownish green from grass green. The precipitate was filtered and washed with $CHCl_3$ to remove excess ligand. The compound was recrystallized from ether/acetonitrile to obtain the pure compound. Yield: 47% (0.30 mmols, 258.6 mg). $[(i\text{-}Pr_2Pipdt)_2MoOCl][MoOCl_4]$, Anal. Calcd (experimental) for $C_{20}H_{36}N_4S_4Mo_2O_2Cl_5$: C, 27.87 (28.72); H, 4.21 (4.32); N, 6.50 (6.73). IR (pure solid), cm^{-}1: *n*(C–N), 1520 (vs), *n*(C=S), 1364 (vs), *ε*(Mo=O), 949 (vs), 904 (m). ESI-MS (MeCN): C_{20} H_{36} N_4S_4MoOCl, *m*/*z* 609 $[M]^+$, $MoOCl_5$ *m*/*z* 253 $[M]^{1-}$. λ_{max}, nm in CH_3CN (*ε*, M^{-1} cm^{-1}): 741 (366), 673 (338), 414 (1239), 313 (11024).

Synthesis of $[(i\text{-}Pr_2Pipdt)_2MoOBF_4][BF_4]$ (1b)—100 mg (0.12 mmoles) of $[(i\text{-}Pr_2Pipdt)_2MoOCl][MoOCl_4]$ was dissolved in 20 ml acetonitrile and stirred for 1 h. To this mixture, 10 equivalents (235 mg) of $AgBF_4$ in 15 mL of acetonitrile was added slowly and the reaction mixture was stirred for 3 h. The color of the solution changed from green to brownish green. AgCl was filtered out *via* micro filtration and the resulting dark brownish green filtrate was dried under vacuum. From the solid residue, excess $AgBF_4$ was extracted with 100 mL of toluene. The pure $[(i\text{-}Pr_2Pipdt)_2MoOBF_4][BF_4]$ was dried in vacuum overnight. Yield: 78% (0.093 mmoles, 70 mg). $C_{20}H_{36}N_4S_4MoOB_2F_8$ + $AgBF_4$ Anal. Calcd, (experimental) for $[(i\text{-}Pr_2Pipdt)_2MoOBF_4][BF_4]$: C, 24.26 (25.53); H, 3.14 (3.86); N, 5.02 (5.95), IR (pure solid) cm^{-1}: *ν*(C(=S)−N), 1505 (vs), *ε*(C=S), 1365 (vs), *ε*(Mo=O), 938 (vs), *ε*(BF_4), 1030 (sh). ESI-MS (MeCN): $C_{20}H_{36}N_4S_4MoOBF_4$, *m*/*z* 661 $[M]^+$ $C_{20}H_{36}N_4S_4MoOF$ *m*/*z* 593, $[M]^+$ ^{1}H NMR (CD_3CN, room temperature): *δ* 5.57, (sep, 2H, CH), 5.42 (sep, 2H, CH), 4.04, (s, 4H, CH_2) 3.48 (s, 4H, CH_2), 1.50, (d, 12H, CH_3, 1.25 (d, 12H, CH_3). ^{13}C NMR (CD_3CN): *δ* 180.62 (C=S) 59.56 (CH), 43.15(CH_2), 18.03 (CH_3). ^{19}F NMR (CD_3CN, referenced to trifluroacetic acid at 280K), *δ* −150.5, 150.6 (coordinated BF_4), *δ* −151.4, −151.5 (free BF_4^-) l_{max} nm in CH_3CN (*ε*, M^{-cm-1}): 718 (910), 411 (2238), 314 (18658).

Synthesis of $[(i\text{-}Pr_2Pipdt)Mo]_4[BF_4]_4$ (2)—300 mg (0.431 mmol) of **1b** was dissolved in 10 mL MeCN, and to this brownish green solution an excess (1:10) pyridine was added resulting in a brown solution. The reaction mixture was stirred for 30 min before filtering. The filtrate was evaporated to dryness and washed several times with ether to remove excess pyridine. The crude product was recrystallized from acetonitrile and ether to obtain the analytically pure compound. Yield: 80% (0.344 mmol, 600 mg). Anal. calcd. For $[(i\text{-}Pr_2Pipdt)Mo]_4[BF_4]_2$, $C_{40}H_{72}N_8S_8Mo_4B_4F_{16}$ C_5H_5N (experimental): C, 31.21 (33.0); H, 4.48 (4.91); N, 7.28(7.58). IR (pure solid) cm^{-1}: *ε*(BF_4), 1030; *ε*(C(=S)–N), 1489; –(C=S), 1362. ^{1}H NMR (CD_3CN): *δ* 5.32, (sep, 2H), 3.44 (sep, 2H), 3.66, (s, 4H), 3.29 (s, 4H), 1.35, (d, 12H), 1.15(d, 12H). ^{19}F NMR (CD_3CN, referenced to trifluoroacetic acid at 280 K), *δ* μ150.3 (coordinated BF_4), *δ* μ151.3, μ151.4 (free BF_4^-) λ_{max},nminCH$_3$CN (*ε*,M^{-}1cm^{-1}): 497(820), 368 (1950), 314 (3920), 254 (18850).

Results and discussion

Synthesis

The desoxo-Mo cluster was synthesized in three steps starting from $MoCl_5$ and the ligand. The synthetic scheme is shown in Scheme 1. The mononuclear oxo-molybdenum(IV) compound, **1a** was synthesized as a green solid in moderate (47%) yield by reacting $MoOCl_3(THF)_2$ with the ligand, i-Pr_2Pipdt. The resulting complex is in the Mo(IV) oxidation state indicating that a part of the starting material is oxidized to Mo(VI), which was not isolated. This also explains the observed yield. Through isotope labeling experiments we have demonstrated that ‘anhydrous’ molybdenum pentachloride readily incorporates a terminal oxo-group from the water molecule present in the system (*e.g.*, residual water in the solvent).[24]

Compound **1b** was synthesized from **1a** *via* chloride substitution reaction with $AgBF_4$ in good (78%) yields. Despite several attempts, $AgBF_4$ could not be completely removed from the product, which is consistent with elemental analyses. In the presence of pyridine, the blue colored acetonitrile solution of compound **1b**, rapidly changed to red-brown from which compound **2** was isolated in excellent (80%) yield. All compounds are soluble in polar solvents such as acetonitrile and acetone but insoluble in non-polar solvents such as benzene, or hexane.

The stoichiometry of the reaction has been determined to be 1:1 (**1b**: pyridine) by Job's method. [25] Upon addition of pyridine the color of the solution changed rapidly to brown, and this color change has been probed by uv-visible spectroscopy. Thus acetonitrile solutions of **1b** were reacted with pyridine resulting in an increase of the peak at 475 nm and decrease of the peak at 740 nm. The titration indicates one mole of pyridine is required for conversion of **1b** to **2**.

The terminal Mo=O bonds are strong because of the electron donation to the Mo d_{Π} orbitals from oxygen resulting in multiple bond character.[26] Thus removal of the terminal oxo-group from a higher valent oxo-Mo center requires the formation of a stronger bond *e.g.*, formation of a P=O bond.[27] Pyridine can also act as an oxo-abstractor forming pyridine *N*-oxide,[28] and can lead to the formation of the desoxo-species. Alternatively, the desoxo-cluster can be formed utilizing methods other than direct oxo-transfer chemistry. Majumdar *et al*. recently reported protonation of a terminal oxo group in an oxo-Mo(IV) complex leading to the formation of a desoxo species, which subsequently formed a trinuclear cluster[29] They suggested that the $\{Mo^{IV}=O\}$ unit behaves like a carbonyl species and can be easily protonated. Carbonyl groups, particularly when coordinated to a metal, are very sensitive to nucleophilic attack[30] due to residual positive charge resulting in a greater metal-to-ligand charge donation. In the present case, we suggest such a situation may exist and the reaction may proceed *via* nucleophilic attack by pyridine. Of course, direct oxo-transfer reaction also proceeds *via* nucleophilic attack by pyridine, although this step is generally very fast.[31] The nucleophilic attack is supported by experiments conducted with pyridines with different basicities. Thus, when compound **1b** was titrated with 4-cyanopyridine (CP), and 4-*N*,*N*-dimethylpyridine (DMAP), the reaction with 4-cyanopyridine proceeded slower than the other two. Such labilization of the terminal oxo-group may be enhanced by the electron donating power of the dithione ligand. Continuing work in our laboratory will further clarify these points.

Crystal structure

The molecular structures of compound **2** and the free ligand (iPr_2Pipdt) have been determined by single crystal X-ray diffractometry. The structure of **2** is shown in Fig. 1, and the crystal data is tabulated in Table 1. In complex **2**, four molybdenum and two sulfur atoms are at the core of the cluster forming a sixmembered ring. Two sulfur atoms of the planar six membered core occupy the opposing sites. In compound **2**, the dithione ligand coordinates the metal center asymmetrically. One of the two sulfur atoms coordinates to one molybdenum atom, while the other sulfur serves as a bridge coordinating to two metal ions. This asymmetric binding is also reflected in the Mo–S bond distances discussed later.

The stereochemical arrangement about the molybdenum centers exhibit two distinct types. One molybdenum center exhibits a distorted tetrahedral geometry while the other one displays a near planar geometry. The molybdenum atoms are coordinated weakly by the fluorine of $[BF_4]^-$ and Mo–F distances are different for the two molybdenum centers −3.200 Å, 3.115 Å (bidententate) and 2.736 Å (monodentate). Both distances are longer than known Mo–FBF_3 distances.[32,33] When the coordination of the $[BF_4]^-$ is considered, the Mo-centers display a distorted trigonal bipyramidal geometry with the three coordinating sulfur are on the equatorial plane. The Mo–Mo–F angle is found to be 140^{δ}, significantly smaller than 180^{δ}. The distorted geometry of the metal center coordinated by the BF_4 anion is shown in Fig. 2. The packing of the cluster shows organized space where the solvent molecule, acetonitrile is packed (Fig. 3).

Important bond lengths and the bond angles are tabulated in Tables 2 and 3. The Mo–S bond distances range from 2.418(1) to 2.611(1) Å; the longer distance is associated with the bridging sulfur. The average Mo–S distance is 2.54 Å which is slightly longer than that observed in (Me Pipdt)Mo(CO) **18** and is longer than the Mo–S(dithiolene) distance. The C=S distances (1.689, 1.694 Å)in **2** are shorter than the C–S single bond distance. The C–S distance in the free ligand is 1.674 Å, thus they do not change significantly upon coordination to a metal ion. Long Mo–S distance and short C=S distances are indicative of the oxidized nature of the ligand. The C(S)–C(S) bond distance in the free ligand is 1.509 Å which is elongated in **2** (1.529 Å and 1.519 Å) by 0.01 Å.

Compared to the bond distances, the S–C–C–S torsion angle shows significant changes upon coordination. In the free ligand the S–C–C–S torsion angle is 36.87° which we believe is due to the flexible methylene backbone of the pipyrazine ring. In Ni(dmit)(i-Pr Pipdt)[34] 2 this angle is reduced to 11.54° and in $Mo(CO)_4$ (Me_2Pipdt)[18] it is reduced to 11.28°. In compound **2** the torsion angle is found to be 27.04° and 37.89°, respectively for the two ligands. Only in one ligand is the torsion angle reduced, by ~10°. Taken together, not only do the two sulfur atoms of the same ligand coordinate differently, but also the ligands are distorted differentially, and the structure of the free ligand is preserved in **2**.

The Mo–Mo distance of 3.02 Å found in **2** is longer than a typical Mo–Mo quadruple bond of 1.9–2.3 Å,[35] and it is even longer than a single bond distance. Mo-Mo distances longer than 3 Å have been reported in binuclear complexes such as $[Mo_2Cp_2(\mu\text{-}H)(\mu\text{-}PHR)(CO)_4]$ (R = Cy, 2,4,5-$C_6H_2R'_3$; R′ = H, Me, ^{t}Bu) where the Mo–Mo distance is reported to be ~3.5=Å.36 In binuclear molybdenum complexes coordinated by bridging sulfur donors Mo–Mo distances ~2.6 Å, have also been reported. Longer distances have also been observed in trinuclear molydenum clusters coordinated by sulfur donors.[37] While there is a precedence of longer distance, the exact nature of the bond (or interaction) is yet to be fully understood. Longer (~3Å) distance is concomitant with the expansion of the Mo–S_b–Mo (S_b being the bridging sulfur) angle to ~82°. In compound **2**, Mo–S_b–Mo is found to be 92°, which is significantly higher to accommodate the larger cluster. Interestingly, the S_b–Mo–Mo angle is found to be 124°, closer to the interior angle for a hexagon. Thus, the structure of the cluster (**2**) is stabilized not only by distortion at the ligand but also an expanded core of the cluster.

Spectroscopic characterization

The molybdenum complexes were characterized by IR, NMR and UV-visible spectroscopies. Compounds **1a, 1b** and **2** exhibit a relatively strong band at ~1364 cm^{-1} due to the *ν*(C=S) vibration. In compound **2**, this band is broader than that found in **1a** or **1b**. In the free ligand this stretch appears at 1344 cm^{-1}. Thus upon coordination the *ν*(C=S) vibration shifts by 20 cm^{-1} to lower frequency. Both **1b** and **2** exhibit a broad strong band at ~1030 cm^{-1} due to the coordinated $[BF_4]^-$ anion. One sharp Mo=O stretch appears at 938 cm^{-1} in compound **1b**, and in compound **1a** two such bands appear at 949 cm^{-1} (from (i-Pr_2Pipdt)$_2$MoOCl)) and at 904 cm^{-1} (from $MoOCl_4$). No such band is observed in **2** indicating the loss of the terminal oxo-group.

The solution properties of the compounds were investigated by NMR spectroscopy. Compound **1a** was, however, not amenable to NMR analysis due to the presence of the paramagnetic counter anion, $[Mo^VOCl_4]$. ^{1}H NMR spectra of the ligand exhibit peaks for CH, CH_2, and the CH_3 groups at 5.39 ppm, 3.42 ppm, and at 1.12 ppm, respectively indicating magnetic equivalence. For **1b**, two sets of resonances were observed, in a 1:4 ratio, for the same groups at slightly different chemical shifts (*δ* 5.57, 5.42 for CH; 4.06, 3.48 for CH_2; 1.50, 1.25 for CH_3. No cross peaks were observed between the two sets in a COSY experiment (data not shown).[19] Therefore we suggest that the two sets may originate from two different geometries about the molybdenum center, due to *cis* and *trans* coordination of the $[BF_4]^-$ with respect to

the Mo=O bond. ^{1}H NMR spectra of **2** exhibits two sets of resonances and one set of signals differing significantly from those of the free ligand. We suggest that this difference may be due to the differential bonding mode of the two sulfur donors of the ligand.

The ^{13}C NMR spectrum is indicative of the redox state of the ligand as C=S and C–S resonate at distinctly different positions. The free ligand, i-Pr_2Pipdt, compounds **1b** and **2** show a peak ~180 ppm suggesting the presence of the C S functionality. In the present case, this peak shifts only modestly (~3 ppm) upon coordination, as was observed for the (Me_2Pipdt)Mo$(CO)_4$ complex.[18] This is different than that observed for the dithiolene coordination where larger up-field shifts (~30 ppm) have been observed for the $(Et_4N_2C_2S_2Mo(PPh_{3)2}(CO)_2$.[38]

We have also probed the coordination of the $[BF_4]^-$ anion by ^{19}F NMR spectroscopy in the temperature range from 296 K to 240 K. Room temperature ^{19}F NMR spectrum of **2** in acetonitrile showed only one resonance at –151.7 ppm, which is similar to that observed for $NaBF_4$ (Fig. 4). At temperatures below 296 K, additional peaks were observed at −149.7 ppm and at −150.3 ppm that are likely to be due to the coordination to the molybdenum center. Also a weak peak was observed at −150.3 ppm at 240 K. Taken together ^{19}F NMR is indicative of a dynamic coordination environment[39] about the molybdenum center which is consistent with the weak coordination of the $[BF_4]^-$ anion found in the crystal structure. ^{19}F NMR spectra of **1b** revealed a similar dynamic environment, although no MeCN coordination was observed in the ^{1}H NMR spectra, suggesting a fast exchange.

Acetonitrile of both complex **1a** and **1b** exhibit low-energy transition at 741 and 718 nm, respectively assigned as d to d transitions. We suggest mixing of the ligand character with the metal as the molar extinction coefficients are higher than those expected for a pure d–d transition. Complex **1a** exhibit another low-energy transition at 673 nm with similar intensity which we suggest due to the $[MoOCl_4]^-$ anion. In complex **2** no such transition could be observed. The detail of the electronic structure leading to these transitions is under investigation and will be reported in the future.

Conclusions

In conclusion, here we disclose the synthesis and characterization of two mononuclear higher valent oxo-molybdenum complexes of oxidized dithione ligand. In the presence of pyridine, a novel multinuclear cluster is formed that has been crystallographically characterized in the solid state and spectroscopically characterized in solution. The weak coordination of $[BF_4]^-$ revealed in the crystal structure was probed by solution ^{19}F NMR spectroscopy.

Acknowledgments

Partial financial support from the National Institutes of Health (GM61555) and an equipment grant from the National Science Foundation (CHE 0614785) are gratefully acknowledged.

References

1. Davison A, Edelstein N, Holm RH, Maki AH. J. Am. Chem. Soc 1963;85:2029.
2. Eisenberg R, Stiefel EI, Rosenberg RC, Gray HB. J. Am. Chem. Soc 1966;88:2874–2876.
3. Schrauzer GN, Meyweg VP. J. Am. Chem. Soc 1962;84:3221.
4. Stiefel, EI. Progress in Inorganic Chemistry. Wiley; 2003. Dithiolene Chemistry: Synthesis, Properties, and Applications.
5. Robertson N, Cronin L. Coord. Chem. Rev 2002;227:93–127.
6. Faulmann C, Cassoux P. Prog. Inorg. Chem 2003;52:399–489.
7. Kato R. Chem. Rev 2004;104:5319–5346. [PubMed: 15535652]

8. Madalan AM, Avarvari N, Fourmigue M, Clerac R, Chibotaru LF, Clima S, Andruh M. Inorg. Chem 2008;47:940–950. [PubMed: 18171056]
9. Llusar R, Triguero S, Vicent C, Sokolov MN, Domercq B, Fourmigue M. Inorg. Chem 2005;44:8937–8946. [PubMed: 16296849]
10. Poder-Guillou S, Schollhammer P, Petillon FY, Talarmin J, Girdwood SE, Muir KW. J. Organomet. Chem 1996;506:321–326.
11. Hilsenbeck SJ, Young VG Jr. McCarley RE. Inorg. Chem 1994;33:1822–1832.
12. Enemark JH, Cooney JJA, Wang J-J, Holm RH. Chem. Rev 2004;104:1175–1200. [PubMed: 14871153]
13. Ikada T, Mizobe Y, Hidai M. Organometallics 2001;20:4441–4444.
14. Tsuge K, Imoto H, Saito T. Inorg. Chem 1992;31:4715–4716.
15. Cotton FA, Daniels LM, Hillard EA, Murillo CA. Inorg. Chem 2002;41:2466–2470. [PubMed: 11978114]
16. Burgmayer SJN. Prog. Inorg. Chem 2003;52:491–537.
17. Holm RH. Coord. Chem. Rev 1990;100:183–221.
18. Nemykin VN, Olsen JG, Perera E, Basu P. Inorg. Chem 2006;45:3557–3568. [PubMed: 16634586]
19. Perera, E. Duquesne University; 2008. Ph.D. Dissertation
20. Isaksson R, Liljefors T, Sandstorm J. J. Chem. Res. Synop 1981:43.
21. Bigoli F, Deplano P, Mercuri ML, Pellinghelli MA, Pilia L, Pintus G, Serpe A, Trogu EF. Inorg. Chem 2002;41:5241–5248. [PubMed: 12354058]
22. Sheldrick, GM. SADABS. University of Göttingen; Germany: 2002.
23. Sheldrick GM. SHELXTL 6.1. 2000
24. Nemykin VN, Basu P. Dalton Trans 2004:1928–1933. [PubMed: 15252579]
25. Job P. Ann. Chim 1928;9:113–203.
26. McNaughton RL, Helton ME, Rubie ND, Kirk ML. Inorg. Chem 2000;39:4386–4387.
27. Nemykin VN, Davie SR, Mondal S, Rubie N, Kirk ML, Somogyi A, Basu P. J. Am. Chem. Soc 2002;124:756–757. [PubMed: 11817943]
28. Lee SC, Holm RH. Inorg. Chim. Acta 381:1166–1176.
29. Majumdar A, Mitra J, Pal K, Sarkar S. Inorg. Chem 2008;47:5360–5364. [PubMed: 18470980]
30. Carbtree, RH. The Organometallic Chemistry of the Transition Metals. John Wiley; New York: 2001.
31. Kail BW, Perez LM, Zaric SD, Millar AJ, Young CG, Hall MB, Basu P. Chem.-Eur. J 2006;12:7501–7509.
32. Day EF, Huffman JC, Folting K, Christou G. Dalton Trans 1997:2837–2841.
33. Weng H-Y, Wu Y-Y, Wu C-P, Chen J-D. Inorg. Chim. Acta 2004;357:1369–1373.
34. Curreli S, Deplano P, Faulmann C, Ienco A, Mealli C, Mercuri ML, Pilia L, Pintus G, Serpe A, Trogu EF. Inorg. Chem 2004;43:5069–5079. [PubMed: 15285683]
35. Collman JP, Woo LK. Proc. Natl. Acad. Sci 1984;81:2592–2596. [PubMed: 16593459]
36. Alvarez CM, Alvarez MA, Garcia-Vivo D, Garcia ME, Ruiz MA, Saez D, Falvello LR, Soler T, Herson P. Dalton Trans 2004:4168–4179. [PubMed: 15573169]
37. Huang JQ, Huang JL, Shang MY, Lu SF, Lin XT, Lin YH, Huang MD, Zhuang HH, Lu JX. Pure Appl. Chem 1988;60:1185–1192.
38. Barnard KR, Wedd AG, Tiekink ERT. Inorg. Chem 1990;29:891–892.
39. Blosser PW, Gallucci JC, Wojcicki A. Inorg. Chem 1992;31:2376–2384.

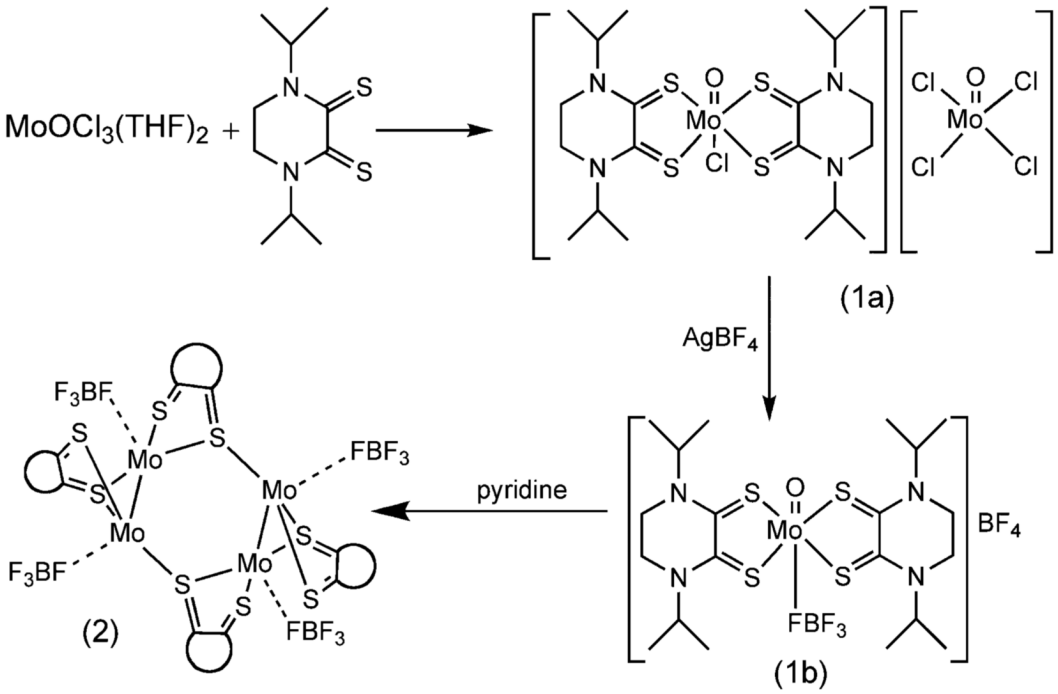

Scheme 1.

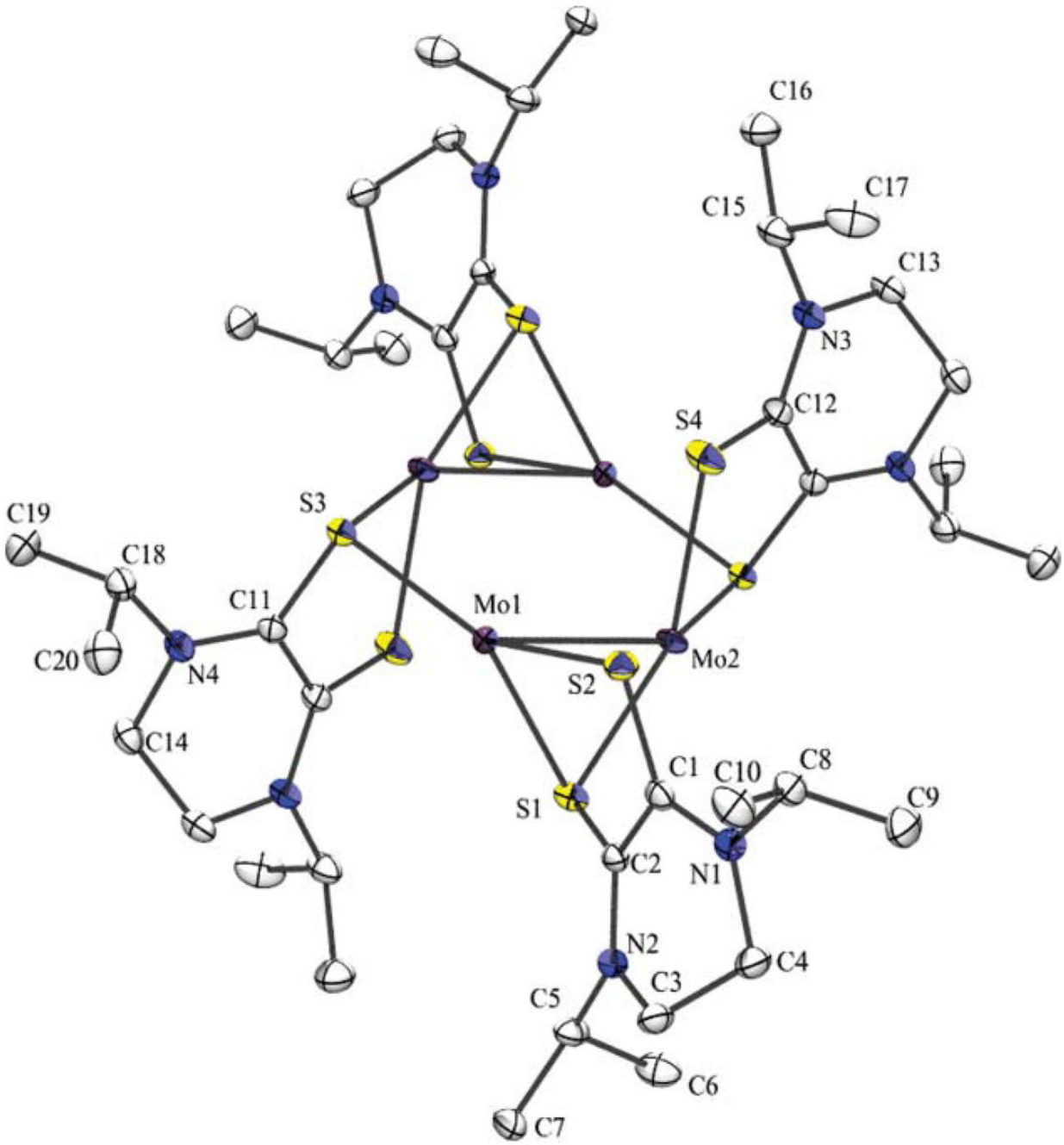

Fig. 1.
Thermal ellipsoid (30%) plot of **2**. The BF_4 anions have been omitted for clarity.

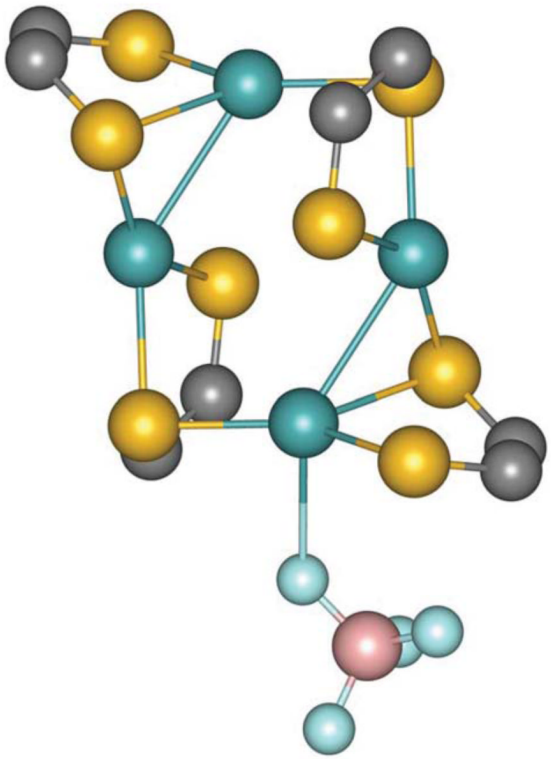

Fig. 2.
Ball and stick model of the core of the cluster showing coordination of the $[BF_4]^-$ anion.

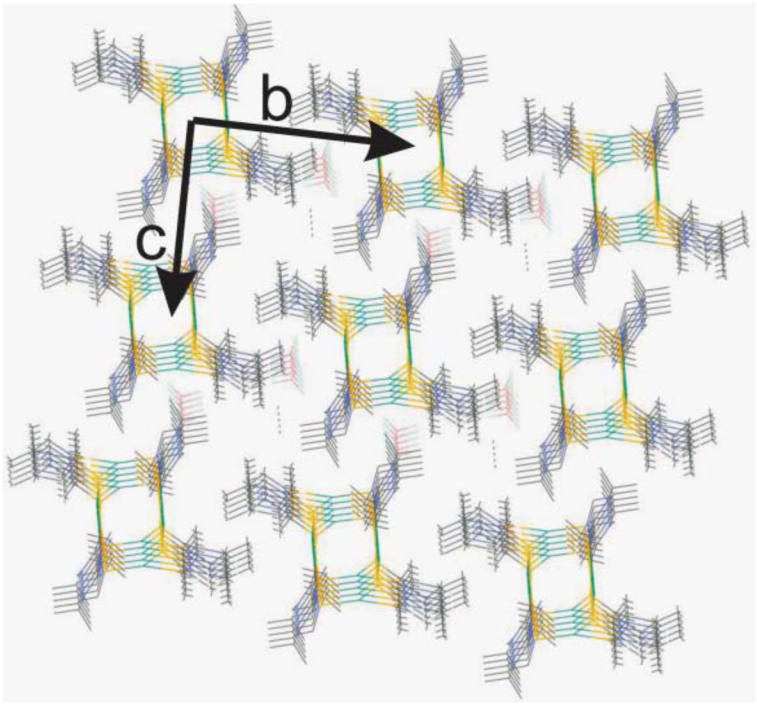

Fig. 3.
Packing diagram of compound **2**. Please note the solvent (acetonitrile) in the open space.

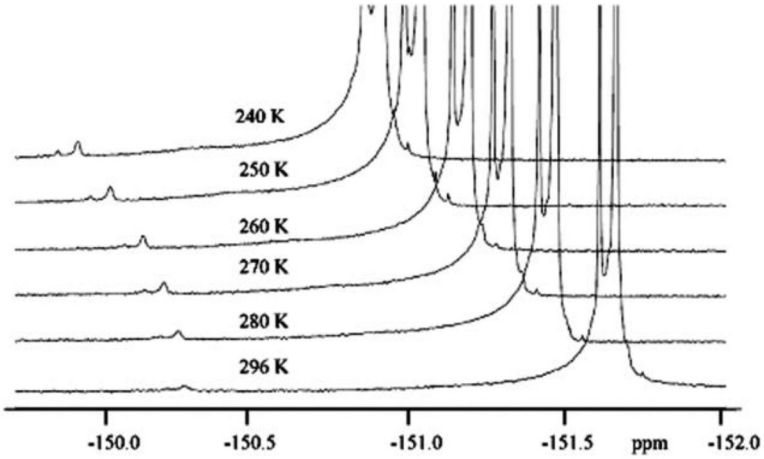

Fig. 4.
^{19}F NMR spectra of acetonitrile solutions of **2** at variable temperature.

Table 1

Crystallographic data[a] for **2**, and i-Pr_2Pipdt ligand

	Compound 2	**i-Pr2Pipdt**
formula	$C_{44}H_{72}Mo_4N_8S_8C_4H_6N_2B_4F_{16}$	$C_{10}\ H_{18}\ N_2\ S_2$
formula weight	1734.64	230.38
T, K	296 (2)	273(2)
crystal system	Triclinic	Monoclinic
space group	*P*-1	*C*2/*c*
a, Å	9.7098(10)	18.5301(7)
b, Å	12.6842(13)	7.0919(3)
c, Å	13.9239(14)	9.7843(4)
α, deg	88.556(2)	90
β, deg	79.629(2)	97.344(3)
γ , deg	83.093(1)	90
Z,	1	4
volume, Å ^{3}	1674.6(3)	1275.24(9)
μ,mm – 1	1.066	0.386
Reflections	16 707	17 607
Unique	6216	1420
R(int)	0.022	0.0945
*R*1	0.0459	0.0828
wR $_2$	0.1397	0.1967
GOF (F^2)	1.085	1.022

[a] Mo K_α radiation. $R1 = \Sigma||F_o| - |F_c||/\Sigma|F_o|$. $wR2 = \{\Sigma\ [w(F_o^2 - F_c^2)^2]/\Sigma\ [w(F_o^2)^2]\}^{1/2}$.

Table 2

Bond lengths (Å) in **2**

Mo(1)–S(1)	2.6114(14)	N(1)–C(8)	1.487(7)
Mo(1)–S(2)	2.4724(14)	C(2)–C(1)	1.529(7)
Mo(1)–S(3)	2.4183(13)	C(6)–C(5)	1.529(9)
Mo(1)–Mo(2)	3.0214(7)	C(8)–C(9)	1.508(8)
Mo(2)–S(1)	2.4605(13)	C(8)–C(10)	1.518(9)
Mo(2)–S(3)	2.5854(13)	C(5)–C(7)	1.520(8)
Mo(2)–S(4)	2.5068(15)	C(11)–N(4)	1.308(7)
S(3)–C(11)	1.723(5)	C(11)–C(12)	1.519(7)
S(3)–Mo(2)	2.5854(13)	C(12)–N(3)	1.328(7)
S(1)–C(2)	1.714(5)	N(4)–C(14)	1.488(7)
S(2)–C(1)	1.694(5)	N(4)–C(18)	1.491(7)
S(4)–C(12)	1.683(5)	N(3)–C(13)	1.475(7)
N(2)–C(2)	1.317(7)	N(3)–C(15)	1.480(7)
N(2)–C(3)	1.463(7)	C(13)–C(14)	1.492(8)
N(2)–C(5)	1.501(7)	C(18)–C(20)	1.517(8)
C(3)–C(4)	1.492(8)	C(18)–C(19)	1.526(9)
N(1)–C(1)	1.314(7)	C(16)–C(15)	1.549(9)
N(1)–C(4)	1.480(7)	C(15)–C(17)	1.525(9)

Table 3

Bond angles (deg) in **2**

S(3)–Mo(1)–S(2)	141.97(5)	S(4)–Mo(2)–Mo(1)	87.94(4)
S(3)–Mo(1)–S(1)	133.77(5)	S(3)–Mo(2)–Mo(1)	143.40(3)
S(2)–Mo(1)–S(1)	84.26(4)	C(11)–S(3)–Mo(1)	97.78(18)
S(3)–Mo(1)–Mo(2)	124.18(3)	C(11)–S(3)–Mo(2)	95.75(17)
S(2)–Mo(1)–Mo(2)	76.36(4)	Mo(1)–S(3)–Mo(2)	92.09(4)
S(1)–Mo(1)–Mo(2)	51.17(3)	C(2)–S(1)–Mo(2)	107.43(17)
S(1)–Mo(2)–S(4)	142.39(5)	C(2)–S(1)–Mo(1)	94.47(17)
S(1)–Mo(2)–S(3)	130.19(4)	Mo(2)–S(1)–Mo(1)	73.06(4)
S(4)–Mo(2)–S(3)	84.17(4)	C(1)–S(2)–Mo(1)	102.66(19)
S(1)–Mo(2)–Mo(1)	55.77(3)	C(12)–S(4)–Mo(2)	103.05(18)